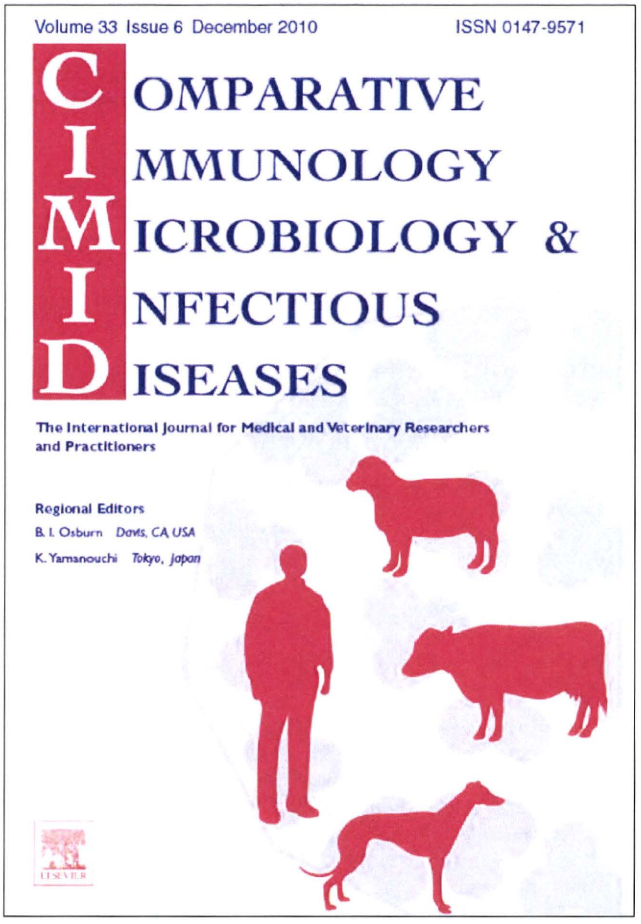

Comparative Immunology, Microbiology and Infectious Diseases 33 (2010) e81–e88

Contents lists available at ScienceDirect

Comparative Immunology, Microbiology and Infectious Diseases

journal homepage: www.elsevier.com/locate/cimid

Evaluation of a recombinant measles virus expressing hepatitis C virus envelope proteins by infection of human PBL-NOD/Scid/Jak3null mouse

Masaaki Satoh[a], Makoto Saito[a], Kohsuke Tanaka[a], Sumako Iwanaga[b], Salem Nagla Elwy Salem Ali[a,d], Takahiro Seki[e,1], Seiji Okada[b], Michinori Kohara[c], Shinji Harada[d], Chieko Kai[e], Kyoko Tsukiyama-Kohara[a,*]

[a] Department of Experimental Phylaxiology, Faculty of Life Sciences, Kumamoto University, 1-1-1 Honjo, Kumamoto-city, Kumamoto 860-8556, Japan
[b] Division of Hematopoiesis, Center for AIDS Research, Kumamoto University, Japan
[c] Department of Microbiology and Cell Biology, Tokyo Metropolitan Institute of Medical Science, Japan
[d] Department of Medical Virology, Faculty of Life Sciences, Kumamoto University, Japan
[e] Laboratory of Animal Research Center, Institute of Medical Science, University of Tokyo, Japan

ARTICLE INFO

Article history:
Received 27 January 2010
Accepted 21 February 2010

Keywords:
MV
HCV
E1
E2
Human PBL
NOD/Scid/Jak3null mouse

ABSTRACT

In this study, we infected NOD/Scid/Jak3null mice engrafted human peripheral blood leukocytes (hu-PBL-NOJ) with measles virus Edmonston B strain (MV-Edm) expressing hepatitis C virus (HCV) envelope proteins (rMV-E1E2) to evaluate the immunogenicity as a vaccine candidate. Although human leukocytes could be isolated from the spleen of mock-infected mice during the 2-weeks experiment, the proportion of engrafted human leukocytes in mice infected with MV (10^3–10^5 pfu) or rMV-E1E2 (10^4 pfu) was decreased. Viral infection of the splenocytes was confirmed by the development of cytopathic effects (CPEs) in co-cultures of splenocytes and B95a cells and verified using RT-PCR. Finally, human antibodies against MV were more frequently observed than E2-specific antibodies in serum from mice infected with a low dose of virus (MV, 10^0–10^1 pfu, and rMV-E1E2, 10^1–10^2 pfu). These results showed the possibility of hu-PBL-NOJ mice for the evaluation of the immunogenicity of viral proteins.

1. Introduction

Hepatitis C virus (HCV) is a member of the *Flaviviridae* family and is the causative agent of both chronic hepatitis and hepatocellular carcinoma (HCC) [1–3]. 170 million people are infected with HCV worldwide [4,5]. Despite prevention efforts and advanced treatment strategies, including combined PEGylated alpha interferron (PEGIFN-α) and ribavirin therapy [6,7], the clinical efficacy of this treatment is limited [8,9]. Alternative novel antiviral agents that have been shown to elicit effective responses in chronically infected patients, such as inhibitors of viral protease, helicase, and polymerase, are currently being developed but are expensive [10]. Therefore, the development of an effective vaccine that either induces the production of high-titer, long-lasting, and cross-reactive neutralising antibodies or induces a cellular immune response is important.

Immunological approaches to control HCV infection have proven to be ineffective, in part because HCV adapts to escape from the host immune system [11]. Furthermore, a high percentage of immunocompetent individuals

* Corresponding author. Tel.: +81 96 373 5560; fax: +81 96 373 55620.
E-mail address: kkohara@kumamoto-u.ac.jp (K. Tsukiyama-Kohara).

[1] Present address: Virology, Shionogi Research Laboratories, Shionogi & Co Ltd, Osaka, Japan.

0147-9571/$ – see front matter © 2010 Elsevier Ltd. All rights reserved.
doi:10.1016/j.cimid.2010.02.006

are infected by HCV despite their ability to mount an active immune response [12]. A preventive HCV vaccine is required to protect unexposed individuals from HCV infection. This vaccine will most likely need to target the viral envelope glycoprotein, E1 and E2, and must also be bivalent, safe, and provide long-lasting protective immunity. To address this challenge, we evaluated the immunogenicity of a live-attenuated recombinant vector derived from the pediatric measles virus (MV) that expresses HCV antigens. The MV vaccine is a well-known, live-attenuated vaccine and has proven to be one of the safest, most stable, and effective human vaccines [13]. This vaccine is produced on a large scale in many countries and used at low cost through the Extended Program on Immunisation of the WHO [14,15]. While this vaccine has been shown to induce life-long immunity with a single dose, boosting is effective. Efforts to develop vaccines using recombinant MV expressing different proteins derived from dengue virus [16,17], human immunodeficiency virus (HIV) [18–21], Human papilloma virus (HPV) [22], Severe acute respiratory syndrome (SARS) [23], or West Nile virus (WNV) [24] have been described. We constructed a recombinant MV expressing the E1 and E2 envelope glycoproteins of HCV (rMV-E1E2) [25] and demonstrated that this virus could infect B95a cells and express HCV E1.

HCV research has long been hampered by the lack of an animal model that reproduces HCV infection in humans. The model in which severe combined immunodeficient (SCID) mice are transplanted with human peripheral blood leukocyte (PBL) is a well-established system to study human immunity (hu-PBL-SCID). This mouse develops all human lymphoid cell lineages that repopulate the animal's lymphoid organs. Our group previously generated the non-obese diabetic (NOD)/SCID/Janus kinase 3 (Jak3) knockout (NOJ) mouse model and then established a human hemolymphoid system in this mouse [26,27]. In this study, we infect human PBL-transplanted NOJ mice with MV and rMV-E1E2 and then characterise the humoral immune responses elicited by the transplanted human cells, in order to evaluate rMV-E1E2 as a vaccine candidate.

2. Materials and methods

2.1. Cells

B95a cells, a marmoset B cell line [28], were used for viral titration and rescue, and were maintained in RPMI 1640 medium supplemented with 10% heat-inactivated foetal calf serum (FCS).

2.2. Plasmid construction and viral rescue

The cDNAs encoding HCV E1 and E2 were obtained from the plasmid HCR6CNS2 [29]. We used replication-competent MV-based vectors (pMV; Edmonston B strain of MV) [25]. The E1 and E2 cDNAs were cloned into the *Fse* I site of pMV and the resulting clone, pMV-E1E2, was used to rescue the infectious recombinant MV expressing the HCV envelope glycoproteins (rMV-E1E2), as reported previously [30].

2.3. Generation of humanised mice

Mice were reconstituted as described previously [26,27]. The NOD/SCID/JAK3^{null} strain was established by backcrossing JAK3^{null} and the NOD Cg-Prkdc^{Scid} strains for ten generations. All animal experiments were performed according to the guidelines of Institutional Animal Committee or Ethics Committee of Kumamoto University.

2.4. Preparation of human blood leukocytes and transplantation

Peripheral blood leukocytes were isolated from blood donors using Ficoll–Hypaque density gradient centrifugation. A total of 5×10^6 cells were transplanted into the spleen of irradiated (2 Gy) 4-week-old mice.

2.5. MV and MV-E1E2 infection

We injected 10^0–10^5 pfu of MV or 10^0–10^2 or 10^4 pfu of MV-E1E2 intraperitoneally for MV and MV-E1E2 infection, respectively. As a negative control, a group of mice was injected with RPMI 1640. Mice were monitored for 2 weeks and then euthanised. The spleens and peripheral blood were collected for analysis.

2.6. Flow cytometry

Isolated splenocytes were stained with APC-Cy7-conjugated anti-mouse CD45 (BD Pharmingen) to detect the murine leukocytes and either APC- or pacific blue-conjugated anti-human CD45 (DAKO) to detect human leukocytes. All data were analysed using FlowJo (Tree Star).

2.7. Confirmation of viral infection

The viral infection of the human leukocytes was confirmed using co-culture with B95a cells followed by RT-PCR. Suspensions of isolated splenocytes were co-cultured with B95a cells and the formation of cytopathic effects (CPEs) was monitored for 2 weeks. Additionally, RNA was isolated from the supernatant of the co-cultures using ISOGEN-LS (Nippon gene) according to manufacturer's instructions. MV RNA was detected using reverse transcript-PCR (RT-PCR) with the sense primer, 5′-ACTCGGTATCACTGCCGAGGATGCAAGGC-3′ (1256–1284) and anti-sense primer 5′-CAGCGTCGTCATCGCTCTCTCC-3′ (2077–2056) or 5′-atggcagaagagcaggcacg-3′ (1807–1826). HCV E1 or E2 was amplified using E1-S-1051 5′-ccgttgctgggtggcactta-3′ and E1-AS-1314 5′-atcatcatgtcccaagccat-3′ or E2-S-1600 5′-ctggcacatcaacaggactg-3′ and E2-AS-1960 5′-aaggagcagcacgtctgtct-3′.

2.8. ELISA

Anti-MV antibody titers were determined by using an ELISA assay. 96-well plates were coated with a 25 μg/ml solution of MV-infected B95a lysate or recombinant E2-expressing baculovirus-infected Sf9 lysate as antigen, respectively. The plates were consecutively incubated with

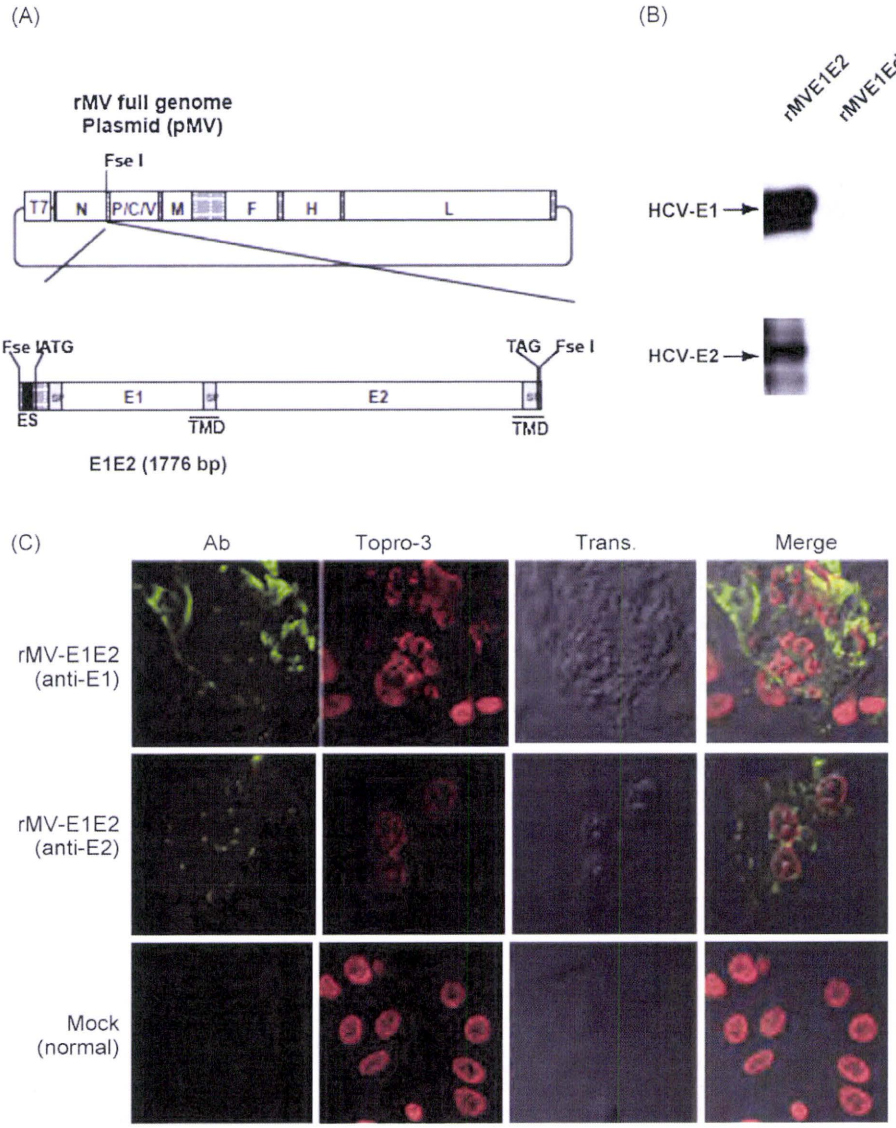

Fig. 1. Construction of the recombinant MV vectors. (A) The rMV full genome vector derived from the MV-Ed strain is illustrated in the upper panel and is labelled with letters as follows: N, nucleocapsid; P, phosphoprotein; M, matrix; F, fusion; H, hemagglutinin; and L, large. T7 indicates the T7 RNA polymerase promoter. The cDNA encoding the HCV envelope glycoproteins (E1 and E2) containing the signal peptide sequence (SP) and the transmembrane domain (TMD, underlined) regions, the N gene end signal (E), the P gene start signal (S), and the intercistronic region of the H protein genes at the 5′ end, which was flanked by Fse I sites at both ends, was introduced into the unique Fse I site in between the N and P genes in the pMV vector. The resulting plasmid was designated pMV-E1E2. (B) The HCV E1 and E2 proteins were detected in rMV-E1E2-, rMV-Ed- and mock-infected B95a cells by western blot with MoAb 384 and 544 (arrows). (C) rMV-E1E2-infected B95a cells were stained with MoAb 299 (anti-E1) or MoAb 187 (anti-E2) and analysed by immunofluorescence. Nuclei were stained with Topro-3 and the bright field and merged images are indicated (400×).

sera (1:100) recovered from hu-PBL-NOJ mice, peroxidase-conjugated rabbit-human IgG (DAKO), and TMB Peroxidase EIA Substrate Kit (Bio-Rad) at 37 °C for 1 h. Optimal density values were measured at 450 nm.

An anti-MV-NP antibody (Millipore, MA, USA) and normal mouse serum (NMS) were used as positive control and negative control respectively.

2.9. Western blot analysis

Total protein extracts from E2-expressing baculovirus-infected Sf9 lysate were separated by SDS-PAGE. The primary antibodies used for Western blots were as follows: sera from mice (1:100) and anti-E2 monoclonal antibody (1:5000). Peroxidase-conjugated secondary antibodies were added and incubated with the mixture for 1 h at room temperature.

3. Results

3.1. Construction of recombinant measles virus expressing E1 and E2

The HCV genes corresponding to the envelope proteins E1 and E2 were sub-cloned in between the N and P genes of the MV vector (Fig. 1A). The HCV E1 and E2 genes included

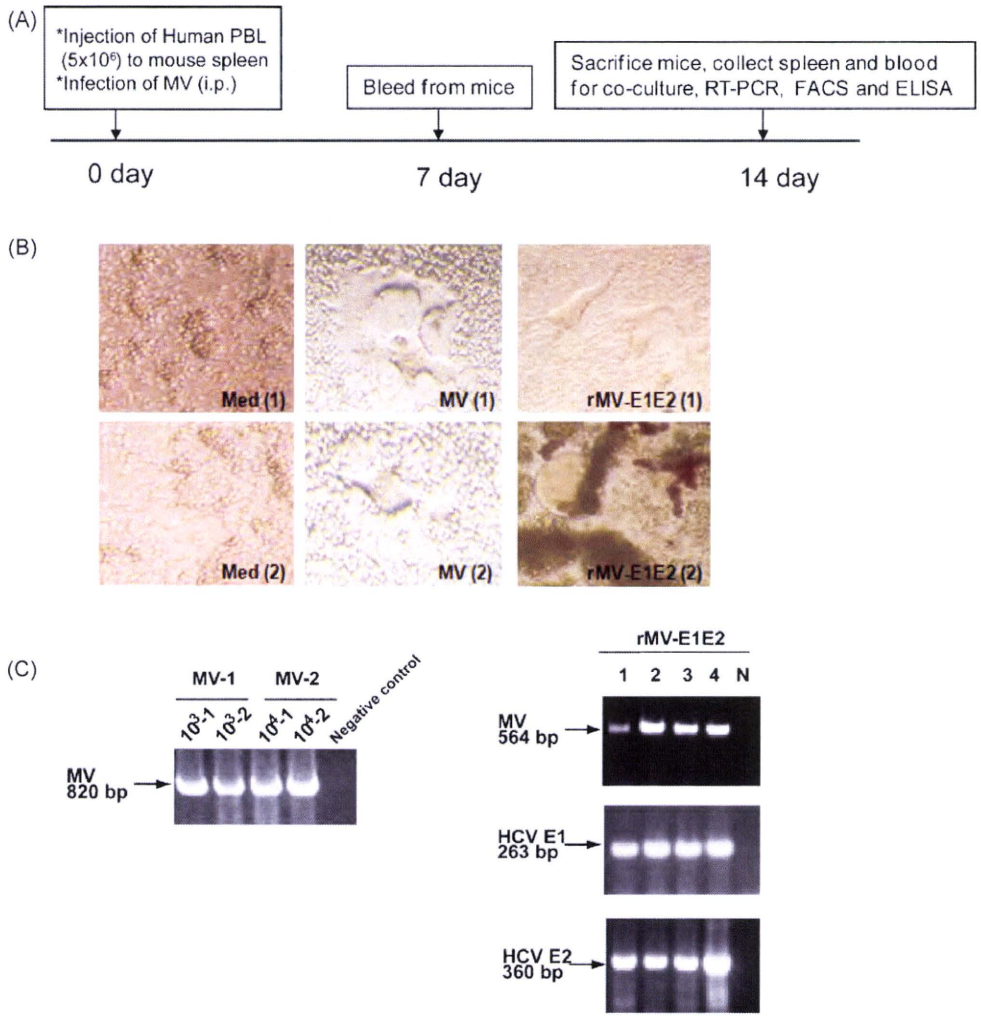

Fig. 2. Infection of hu-PBL-NOD/Scid mice with rMV and rMV-E1E2. (A) Course of infection of hu-PBL-NOD/SCID mice with MV and rMV-E1E2. (B) CPE formation in co-cultures of splenocytes isolated from MV- (MV1, 2), rMV-E1E2-, or mock-infected hu-PBL-NOD/SCID and B95a cells (40× magnification). (C) Detection of viral RNA by RT-PCR. Detection of MV in MV-1- or 2-infected mouse splenocyte co-cultures (820 bp) and rMV-E1E2-infected splenocyte co-cultures (564 bp), and HCV E1 (263 bp) and E2 (360 bp) in rMV-E1E2 (10^4 pfu)-infected splenocyte co-cultures (arrows).

the putative signal peptide sequences at the N terminus and the transmembrane domain at the C terminus [31]. The plasmid vector pMV-E1E2 was introduced with supporting plasmids into 293T cells to rescue the recombinant viruses. The expression of the E1 and E2 proteins by rMV-E1E2 was examined by Western blot (Fig. 1B) and immunofluorescence (Fig. 1C).

3.2. Infection of hu-PBL-NOJ mice with MV and rMV-E1E2

All hu-PBL-NOJ mouse infections were observed for 14 days (Fig. 2A). Infections with MV and rMV-E1E2 were confirmed by first co-culturing the human leukocytes isolated from the spleens of infected mice with B95a cells and then verifying the presence of virus by RT-PCR. In all the MV (10^3–10^4 pfu) or rMV-E1E2 (10^4 pfu)-infected hu-PBL-NOJ mice, CPEs were observed in co-cultures with splenocytes (Table 1; Fig. 2B). The results of the co-culture assays are in agreement with results that were obtained by RT-PCR; positive bands were observed in the mice infected with 10^3–10^4 pfu of MV and 10^4 pfu of rMV-E1E2 (Fig. 2C). These results demonstrate that the rescued MV and rMV-E1E2 are able to infect transplanted human PBL.

Table 1
Summary of MV and MV-E1E2 infection of hu-PBL-NOJ mice.

Virus	Amount of virus (PFU)	No. tested	CPE	RT-PCR
Mock	Medium	7	0/7	0/7
MV	10^0	3	0/3	0/3
	10^1	3	0/3	0/3
	10^2	3	0/3	0/3
	10^3	2	2/2	2/2
	10^4	2	2/2	2/2
MV-E1E2	10^0	3	0/3	0/3
	10^1	3	0/3	0/3
	10^2	3	0/3	1/3
	10^4	4	4/4	4/4

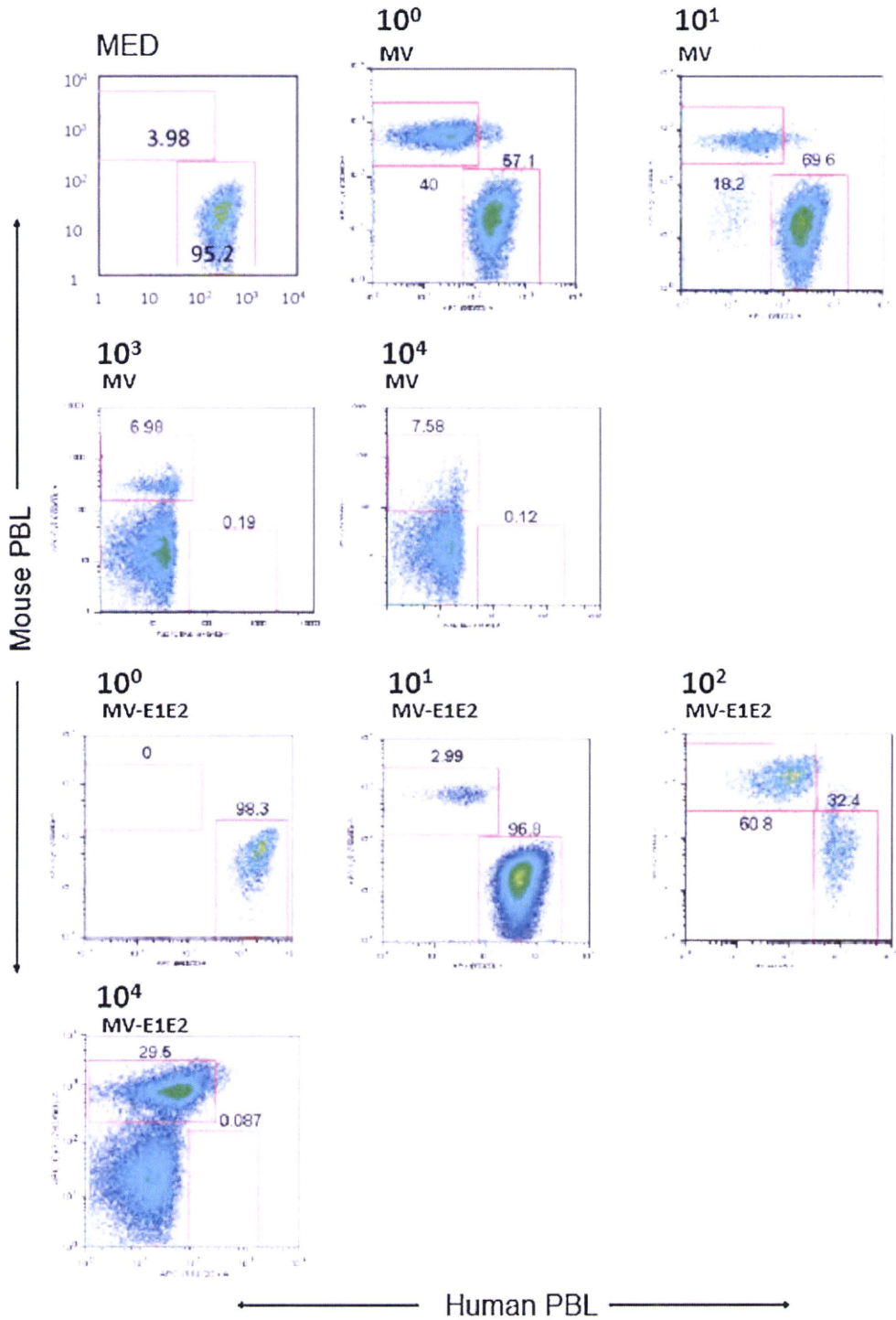

Fig. 3. Flow cytometric analysis of splenocytes isolated from hu-PBL-NOJ mice inoculated with medium, MV-Ed (10^0–10^4 pfu), or rMV-E1E2 (10^0–10^2 or 10^4 pfu). Splenocytes, consisting of both human and murine cells, were stained with antibodies against human or mouse CD45. Representative flow cytometric profiles of each group of infected mice are shown. The percentages of mouse and human leukocytes are shown.

3.3. Proportion of engrafted human leukocytes in MV- and rMV-E1E2- infected hu-PBL-NOJ mice

We also examined the splenocytes of infected mice simultaneously, using flow cytometry to determine the proportion of human cells in the spleen (Fig. 3, Table 2). In the MV-infected hu-PBL-NOJ mice, a population of human leukocytes was observed in the mice that were infected with 10^0–10^1 pfu, whereas few human leukocytes were observed in mice infected with 10^2–10^4 pfu. In contrast, in the rMV-E1E2-infected mice, a population of human leukocytes was detected in mice that were inoculated with 10^0–10^2 pfu. The ratio of human leukocytes settlement in both groups of mice was inversely correlated

Table 2
Proportion of human peripheral leukocytes in the spleen of MV-, rMV-E1E2, or mock-infected hu-PBL-NOJ mice.

Virus	Amount of virus (PFU)	No. tested	huPBL settlement (average ± S.D.%)
Mock	Medium	6	90.9 ± 13.1
MV	10^0	3	92.7 ± 11.2
	10^1	3	58.4 ± 50.6
	10^2	3	55.1 ± 49.9
	10^3	4	4.9 ± 6
	10^4	2	1.7
MV-E1E2	10^0	2	79.6
	10^1	2	96.0
	10^2	3	56.2 ± 36.2
	10^4	3	0.34 ± 0.4

with the results from the RT-PCR and co-culture assays (Table 1).

3.4. Humoral response of MV- and rMV-E1E2-infected hu-PBL-NOJ mice

To examine the immune response against MV and rMV-E1E2 by the transplanted human PBLs, we measured human MV- or HCV-specific antibodies using an ELISA with an MV-infected B95a cell lysate (Fig. 4A) or recombinant HCV E2 protein (Fig. 4B). A significant amount of human antibody against MV antigens was detected in the sera from mice that were infected with MV (10^0–10^1 pfu) or rMV-E1E2 (10^1–10^2 pfu) (Fig. 4A and B). However, only one mouse, which was infected with 10^2 pfu of rMV-E1E2, generated human antibodies against HCV E2 (Fig. 5A). The antibody responses in this mouse were confirmed by Western blot analysis (Fig. 5B).

4. Discussion

The development of a vaccine against HCV has relied on several tools, including recombinant proteins and peptides that are derived from HCV antigens [12,32–34]. HCV E1 E2 proteins play essential roles in the entry of HCV into host cells. Therefore, these proteins represent ideal targets for neutralising antibodies to block viral entry.

Several studies have used the measles virus as a vector for expression of other viral proteins [16,17]. In this study, we examined the infectivity of a rescued Edmonston B strain of MV and a recombinant rMV-E1E2 that was constructed using reverse genetics [25,30]. We demonstrate that these viruses can infect hu-PBL-NOJ mice. This is the first report demonstrating that rescued virus, including a recombinant virus, can infect hu-PBL-NOJ mice. Furthermore, an adequate viral titer could control the generation of antibodies in these mice. Based on the flow cytometry data, most of the human leukocytes disappeared following infection with high virus titer (10^3–10^4 pfu) and human antibody was not detected in these mice (data not shown). In contrast, a population of human leukocytes was detected in the mice that were inoculated with a lower dose of virus (10^0–10^2 pfu). In addition, we could detect human antibodies in the serum of mice that were infected with a low dose of virus, suggesting that this viral titer range is suitable for the induction of an antibody response that targets rMVs in the hu-PBL-NOJ mouse system. This range of virus concentration is adequate for antibody production and the resulting antibody response might suppress the viral growth of 10^0–10^1 pfu MVs in hu-PBL-NOJ mice.

The humanised mouse is a promising model for studying the transmission of the live, attenuated Edmonston B strain of the measles virus. There have been several reports detailing the infection of experimental transgenic mice that

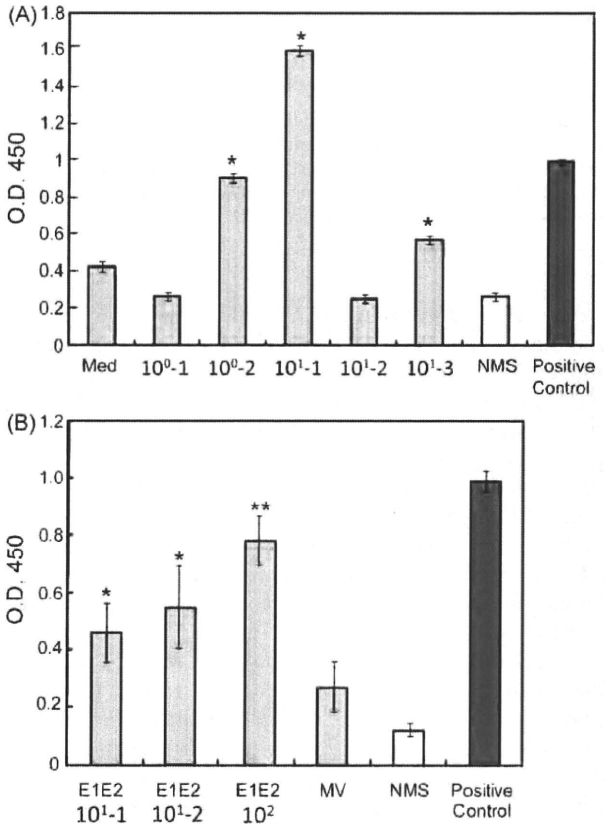

Fig. 4. Detection of human MV-specific antibodies in the serum of rMV- or rMV-E1E2-infected mice. (A) Serum (1:100) from MV-infected mice (10^0–10^1 pfu) was analysed by ELISA using an MV-infected B95a cell lysate as the target. An anti-MV-NP antibody was used as a positive control and NMS indicates normal mouse serum. The asterisk (*) indicates a significant reaction ($p < 0.01$) compared to the medium alone control. (B) Serum (1:100) from rMV-E1E2-infected mice (10^1–10^2 pfu) was analysed by ELISA. An anti-MV-NP antibody was used as a positive control and NMS indicates normal mouse serum. The double asterisk (**) indicates a highly significant reaction ($p < 0.001$) compared to NMS and a single asterisk (*) indicates a significant reaction ($p < 0.05$) compared to NMS.

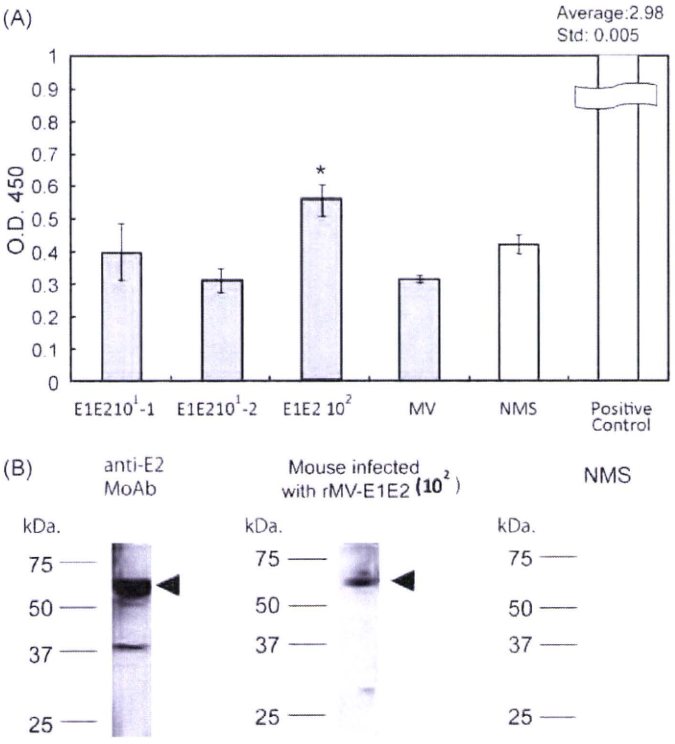

Fig. 5. Detection of E2-specific antibodies using ELISA and western blot. (A) Baculovirus-expressed E2 protein was used as the ELISA antigen and serum (diluted 1:100) from rMV-E1E2-infected mice (10^1–10^2 pfu) was analysed. Anti-E2 monoclonal antibody (MoAb 544) was used as positive control. The asterisk (*) indicates a significant reaction ($p < 0.05$) compared to NMS. (B) An anti-E2 monoclonal antibody (MoAb 544), serum from rMV-E1E2 infected mice (1:100), or normal mouse serum (1:100) was used as primary antibodies in a western blot to detect baculovirus-expressed E2 protein. The triangles indicate bands that correspond to HCV E2.

expresses human CD46 and CD150 with some strains of measles virus [35,36]. However, unlike in other animal models, a population of human cells is the target of the virus in this study. Furthermore, the use of hu-PBL-NOJ mice allows one to monitor the immune response that is generated by human leukocytes against the immunogen. Based on our results, hu-PBL-NOJ mice should be a useful tool for studying the immune response during early MV or rMV-E1E2 infection. Since there is no animal model of HCV infection, monitoring the immune response of human leukocytes permits the accurate evaluation of potential vaccine candidates.

We detected a significant amount of MV-specific antibodies in the rMV-E1E2-infected mice ($n = 3$). However, only one mouse produced E2-specific antibodies and no mice produced E1-specific antibodies. This result could be explained by the hypothesis that the immunogenicity of the E1 and E2, especially E1 protein might be lower than the immunogenicity of the MV proteins, an observation that is consistent with previous studies [37–40].

Further development of the hu-PBL-NOJ mouse model system will allow us to characterise not only the immediate immune response, but also the long-term evolution of the human immune response against measles virus and recombinant measles viruses. This system will make it possible to evaluate the immunogenicity of potential vaccine targets using human PBLs, which is indispensable for the development of an effective vaccine of HCV.

Acknowledgements

We would like to thank Drs. M.A. Billeter and K. Takeuchi for providing the MV Edmonston B strain rescue system, F. Ikeda and M. Yoneda for their technical support. This work was supported by grants from the Ministry of Health and Welfare of Japan, the Ministry of Education, Culture, Sports, Science and Technology of Japan, the Program for Promotion of Fundamental Studies in Health Sciences of the National Institute of Biomedical Innovation, and the Cooperative Research Project on Clinical and Epidemiological Studies of Emerging and Re-emerging Infectious Diseases.

References

[1] Di Bisceglie AM, Carithers Jr RL, Gores GJ. Hepatocellular carcinoma. Hepatology 1998;28(4):1161–5.
[2] Hayashi J, et al. Hepatitis C virus and hepatocarcinogenesis. Intervirology 1999;42(2–3):205–10.
[3] Michielsen PP, Francque SM, van Dongen JL. Viral hepatitis and hepatocellular carcinoma. World J Surg Oncol 2005;3:27.
[4] Global surveillance and control of hepatitis C. Report of a WHO Consultation organized in collaboration with the Viral Hepatitis Prevention Board, Antwerp, Belgium. J Viral Hepat, 1999;6(1):35–47.
[5] Zoulim F, et al. Clinical consequences of hepatitis C virus infection. Rev Med Virol 2003;13(1):57–68.
[6] Bruchfeld A, et al. Ribavirin treatment in dialysis patients with chronic hepatitis C virus infection—a pilot study. J Viral Hepat 2001;8(4):287–92.
[7] Mazzella G, et al. Alpha interferon treatment may prevent hepatocellular carcinoma in HCV-related liver cirrhosis. J Hepatol 1996;24(2):141–7.

[8] Kohara M, et al. Hepatitis C virus genotypes 1 and 2 respond to interferon-alpha with different virologic kinetics. J Infect Dis 1995;172(4):934–8.
[9] Nakamura H, et al. Interferon treatment for patients with chronic hepatitis C infected with high viral load of genotype 2 virus. Hepatogastroenterology 2002;49(47):1373–6.
[10] Bukh J, et al. Studies of hepatitis C virus in chimpanzees and their importance for vaccine development. Intervirology 2001;44(2–3):132–42.
[11] Bowen DG, Walker CM. Mutational escape from CD8+ T cell immunity: HCV evolution, from chimpanzees to man. J Exp Med 2005;201(11):1709–14.
[12] Lechmann M, Liang TJ. Vaccine development for hepatitis C. Semin Liver Dis 2000;20(2):211–26.
[13] Combredet C, et al. A molecularly cloned Schwarz strain of measles virus vaccine induces strong immune responses in macaques and transgenic mice. J Virol 2003;77(21):11546–54.
[14] Naniche D, et al. Decrease in measles virus-specific CD4 T cell memory in vaccinated subjects. J Infect Dis 2004;190(8): 1387–95.
[15] Ovsyannikova IG, et al. Frequency of measles virus-specific CD4+ and CD8+ T cells in subjects seronegative or highly seropositive for measles vaccine. Clin Diagn Lab Immunol 2003;10(3):411–6.
[16] Brandler S, et al. Pediatric measles vaccine expressing a dengue antigen induces durable serotype-specific neutralizing antibodies to dengue virus. PLoS Negl Trop Dis 2007;1(3):e96.
[17] Brandler S, Tangy F. Recombinant vector derived from live attenuated measles virus: potential for flavivirus vaccines. Comp Immunol Microbiol Infect Dis 2008;31(2–3):271–91.
[18] Guerbois M, et al. Live attenuated measles vaccine expressing HIV-1 Gag virus like particles covered with gp160DeltaV1V2 is strongly immunogenic. Virology 2009;388(1):191–203.
[19] Liniger M, et al. Recombinant measles viruses expressing single or multiple antigens of human immunodeficiency virus (HIV-1) induce cellular and humoral immune responses. Vaccine 2009;27(25–26):3299–305.
[20] Lorin C, et al. A recombinant live attenuated measles vaccine vector primes effective HLA-A0201-restricted cytotoxic T lymphocytes and broadly neutralizing antibodies against HIV-1 conserved epitopes. Vaccine 2005;23(36):4463–72.
[21] Lorin C, et al. A single injection of recombinant measles virus vaccines expressing human immunodeficiency virus (HIV) type 1 clade B envelope glycoproteins induces neutralizing antibodies and cellular immune responses to HIV. J Virol 2004;78(1):146–57.
[22] Cantarella G, et al. Recombinant measles virus-HPV vaccine candidates for prevention of cervical carcinoma. Vaccine 2009; 27(25–26):3385–90.
[23] Liniger M, et al. Induction of neutralising antibodies and cellular immune responses against SARS coronavirus by recombinant measles viruses. Vaccine 2008;26(17):2164–74.
[24] Despres P, et al. Live measles vaccine expressing the secreted form of the West Nile virus envelope glycoprotein protects against West Nile virus encephalitis. J Infect Dis 2005;191(2):207–14.
[25] Radecke F, et al. Rescue of measles viruses from cloned DNA. EMBO J 1995;14(23):5773–84.
[26] Okada S, et al. Early development of human hematopoietic and acquired immune systems in new born NOD/Scid/Jak3null mice intrahepatic engrafted with cord blood-derived CD34+ cells. Int J Hematol 2008;88(5):476–82.
[27] Hattori S, et al. Potent activity of a nucleoside reverse transcriptase inhibitor, 4'-ethynyl-2-fluoro-2'-deoxyadenosine, against human immunodeficiency virus type 1 infection in a model using human peripheral blood mononuclear cell-transplanted NOD/SCID Janus kinase 3 knockout mice. Antimicrob Agents Chemother 2009;53(9):3887–93.
[28] Kobune F, Sakata H, Sugiura A. Marmoset lymphoblastoid cells as a sensitive host for isolation of measles virus. J Virol 1990;64(2):700–5.
[29] Tsukiyama-Kohara K, et al. Activation of the CKI-CDK-Rb-E2F pathway in full genome hepatitis C virus-expressing cells. J Biol Chem 2004;279(15):14531–41.
[30] Yoneda M, et al. Rinderpest virus phosphoprotein gene is a major determinant of species-specific pathogenicity. J Virol 2004;78(12):6676–81.
[31] Op De Beeck A, Cocquerel L, Dubuisson J. Biogenesis of hepatitis C virus envelope glycoproteins. J Gen Virol 2001;82(Pt 11):2589–95.
[32] Beyene A, et al. Hepatitis C virus envelope glycoproteins and potential for vaccine development. Vox Sang 2002;83(Suppl 1):27–32.
[33] Seong YR, et al. Immunogenicity of the E1E2 proteins of hepatitis C virus expressed by recombinant adenoviruses. Vaccine 2001;19(20–22):2955–64.
[34] Stamataki Z, et al. Hepatitis C virus envelope glycoprotein immunization of rodents elicits cross-reactive neutralizing antibodies. Vaccine 2007;25(45):7773–84.
[35] Ohno S, et al. Measles virus infection of SLAM (CD150) knockin mice reproduces tropism and immunosuppression in human infection. J Virol 2007;81(4):1650–9.
[36] Sellin CI, et al. High pathogenicity of wild-type measles virus infection in CD150 (SLAM) transgenic mice. J Virol 2006;80(13):6420–9.
[37] Falkowska E, et al. Hepatitis C virus envelope glycoprotein E2 glycans modulate entry, CD81 binding, and neutralization. J Virol 2007;81(15):8072–9.
[38] Helle F, et al. The neutralizing activity of anti-hepatitis C virus antibodies is modulated by specific glycans on the E2 envelope protein. J Virol 2007;81(15):8101–11.
[39] Jackson P, et al. Reactivity of synthetic peptides representing selected sections of hepatitis C virus core and envelope proteins with a panel of hepatitis C virus-seropositive human plasma. J Med Virol 1997;51(1):67–79.
[40] Hoofnagle JH. Course and outcome of hepatitis C. Hepatology 2002;36(5 Suppl 1):S21–9.

Murakami et al. BMC Medical Genomics 2010, 3:48
http://www.biomedcentral.com/1755-8794/3/48

BMC Medical Genomics

RESEARCH ARTICLE Open Access

Hepatic microRNA expression is associated with the response to interferon treatment of chronic hepatitis C

Yoshiki Murakami[1*], Masami Tanaka[2], Hidenori Toyoda[3], Katsuyuki Hayashi[4], Masahiko Kuroda[2], Atsushi Tajima[5], Kunitada Shimotohno[6]

Abstract

Background: HCV infection frequently induces chronic liver diseases. The current standard treatment for chronic hepatitis (CH) C combines pegylated interferon (IFN) and ribavirin, and is less than ideal due to undesirable effects. MicroRNAs (miRNAs) are endogenous small non-coding RNAs that control gene expression by degrading or suppressing the translation of target mRNAs. In this study we administered the standard combination treatment to CHC patients. We then examined their miRNA expression profiles in order to identify the miRNAs that were associated with each patient's drug response.

Methods: 99 CHC patients with no anti-viral therapy history were enrolled. The expression level of 470 mature miRNAs found their biopsy specimen, obtained prior to the combination therapy, were quantified using microarray analysis. The miRNA expression pattern was classified based on the final virological response to the combination therapy. Monte Carlo Cross Validation (MCCV) was used to validate the outcome of the prediction based on the miRNA expression profile.

Results: We found that the expression level of 9 miRNAs were significantly different in the sustained virological response (SVR) and non-responder (NR) groups. MCCV revealed an accuracy, sensitivity, and specificity of 70.5%, 76.5% and 63.3% in SVR and non-SVR and 70.0%, 67.5%, and 73.7% in relapse (R) and NR, respectively.

Conclusions: The hepatic miRNA expression pattern that exists in CHC patients before combination therapy is associated with their therapeutic outcome. This information can be utilized as a novel biomarker to predict drug response and can also be applied to developing novel anti-viral therapy for CHC patients.

Background

Hepatitis C virus (HCV) infection affects more than 3% of the world population. HCV infection frequently induces chronic liver diseases ranging from chronic hepatitis (CH) C, to liver cirrhosis (LC) and hepatocellular carcinoma (HCC) [1]. The current standard treatment for CHC combines pegylated interferon (Peg-IFN) and ribavirin, and has been found to be effective in only 50% of HCV genotype 1b infection. Furthermore this form of therapy is often accompanied by adverse effects; therefore, there is a pressing need to develop alternative strategies to treat CHC and to identify patients that will not be responsive to treatment [2].

MicroRNAs (miRNAs) are endogenous small non-coding RNAs that control gene expression by degrading or suppressing the translation of target mRNAs [3,4]. There are currently 940 identifiable human miRNAs (The miRBase Sequence Database – Release 15.0). These miRNAs can recognize hundreds of target genes with incomplete complementary over one third of human genes appear to be conserved miRNA targets [5,6]. miRNA can associate not only several pathophysiologic events but also cell proliferation and differentiation.

However, there are many miRNAs whose functions are still unclear. Examples include miR-122 which is an abundant liver-specific miRNA that is said to constitute

* Correspondence: ymurakami@genome.med.kyoto-u.ac.jp
[1]Center for Genomic Medicine, Kyoto University Graduate School of Medicine, 53 Shogoinkawahara-cho, Sakyo-ku, Kyoto 606-8507, Japan
Full list of author information is available at the end of the article

up to 70% of all miRNA molecules in hepatocytes [7]. The expression level of miR-122 was reportedly associated with early response to IFN treatment, while others like miR-26 have expression status that is associated with HCC survival and response to adjuvant therapy with IFN [8,9]. IFN beta (IFNβ) on the other hand, has been shown to rapidly modulate the expression of numerous cellular miRNAs, and it has been demonstrated that 8 IFNβ-induced miRNAs have sequence-predicted targets within the hepatitis C virus (HCV) genomic RNA [10]. Finally several miRNAs have been recognized as having target sites in the HCV genome that inhibits viral replication [10-12].

To date, various parameters have been examined in an attempt to confirm the effects of the IFN-related treatment for CHC. In patients with chronic HCV genotype 1b infection, there is a substantial correlation between responses to IFN and mutation in the interferon sensitivity determining region (ISDR) of the viral genome [13]. Substitutions of amino acid in the HCV core region (aa 70 and aa 91) were identified as predictors of early HCV-RNA negativity and several virological responses, including sustained response to standard combination therapy [14]. In order to assess the drug response to combination therapy for CHC using gene expression signatures, several researchers cataloged the IFN related gene expression profile from liver tissue or peripheral blood mononuclear cells (PBMC) [15,16]. It was found that failed combination therapy was associated with up-regulation of a specific set of IFN-responsive genes in the liver before treatment [17]. Additional reports have indicated that two SNPs near the gene IL28B on chromosome 19 may also be associated with a patient's lack of response to combination therapy [18]. These reports suggest that gene expression during the early phase of anti-HCV therapy may elucidate important molecular pathways for achieving virological response [19].

Our aim in this study was to identify gene related factors that contribute to poor treatment response to combination therapy for CHC. In order to achieve this we studied the miRNA expression profile of CHC patients before treatment with CHC combination therapy and tried to determine the miRNAs that were associated with their drug response. Knowing patients' expression profile is expected to provide a clearer understanding of how aberrant expression of miRNAs can contribute to the development of chronic liver disease as well as aid in the development of more effective and safer therapeutic strategies for CHC.

Methods

Patients and sample preparation

Ninety-nine CHC patients with HCV genotype 1b were enrolled (Table 1). Patients with autoimmune hepatitis, or alcohol-induced liver injury, or hepatitis B virus-associated antigen/antibody or anti-human immunodeficiency virus antibody were excluded. There were no patients who received IFN therapy or immunomodulatory therapy before enrollment in the study. Serum HCV RNA was quantified before IFN treatment using Amplicor-HCV Monitor Assay (Roche Molecular Diagnostics Co., Tokyo, Japan). Liver biopsy specimen was collected from each patient up to one week prior to administering combination therapy. Histological grading and staging of liver biopsy specimens from the CHC patients were performed according to the Metavir classification system. Pretreatment blood tests were conducted to determine each patient's level of aspartate aminotransferase, alanine aminotransferase, total bilirubin, alkaline phosphatase, gamma-glutamyl transpeptidase, white blood cell (WBC), platelets, and hemoglobin. Written informed consent was obtained from all of the patients or their guardians and provided to the Ethics Committee of the Graduate School of Kyoto University, who approved the conduct of this study in accordance with the Helsinki Declaration.

Table 1 Clinical characteristics of patients

Characteristics	SVR (n = 46)	R (n = 28)	NR (n = 25)	p-value
Age (years)	57.0 ± 9.8	61.2 ± 8.3	60.6 ± 7.6	0.09†
Male (%)	28 (61%)	11 (39%)	9 (36%)	0.08§
Weight (kg)	59.5 ± 9.0	56.6 ± 9.9	56.0 ± 7.7	0.13†
HCV RNA ($\times 10^6$ copies/ml)	1.90 ± 1.95	1.83 ± 1.04	1.58 ± 0.93	0.62†
Fibrosis stage				0.50§
F 0	1	1	1	
F 1	29	16	10	
F 2	10	7	6	
F 3	6	4	7	
F 4	0	0	1	
WBC($\times 10^3$/mm^3)	5.31 ± 1.59	5.18 ± 1.24	4.71 ± 1.15	0.29†
Hemoglobin (g/dl)	14.2 ± 1.26	13.6 ± 1.35	13.5 ± 1.13	0.022†
Platelet ($\times 10^4$/mm^3)	16.7 ± 5.0	16.4 ± 4.0	15.2 ± 6.1	0.25†
AST (IU/L)	54.8 ± 48.1	46.6 ± 29.3	57.0 ± 28.5	0.17†
ALT (IU/L)	74.5 ± 87.8	47.9 ± 28.6	67.6 ± 43.2	0.15†
γGTP (IU/L)	56.0 ± 69.4	38.5 ± 28.9	74.3 ± 59.0	0.025†
ALP (IU/L)	248 ± 71.5	245 ± 75.7	323 ± 151	0.038†
Total Bilirubin (mg/dl)	0.67 ± 0.22	0.72 ± 0.30	0.68 ± 0.19	0.95†
Albumin (g/dl)	4.21 ± 0.31	4.13 ± 0.27	4.01 ± 0.48	0.14†

Abbreviations. SVR, sustained virological response; R, relapse; NR, non responder; Differences in clinical characteristics among three groups were tested using †Kruskal-Wallis test, or §Fisher's exact test. AST, aspartate aminotransferase; ALT, alanine aminotransferase; WBC, white blood cell; ALP, alkaline phosphatase; γGTP, gamma-glutamyl transpeptidase.

Treatment protocol and definitions

All enrolled patients were treated with pegylated IFNa-2b (Schering-Plough Corporation, Kenilworth, NJ, USA) and ribavirin (Schering-Plough) for 48 weeks (Figure 1). Pegylated IFN was administered at a dose of 1.5 mg kg/week at the starting point. Ribavirin was administered following the dose recommended by the manufacturer.

Definitions of drug response to therapy

Drug response was defined according to how much HCV RNA had decreased in each patient's serum. After four weeks of drug administration (rapid response phase) the patients were classified into the following two groups after four weeks of drug administration: (i) rapid virological responder (RVR): a patient whose serum was negative for serum HCV RNA at four weeks, and (ii) non-RVR: a patient who was not classified as RVR.

The patients were classified into the following three groups after 12 weeks of drug administration (early response phase): (i) complete early virological responder (cEVR): a patient who was negative for serum HCV RNA at 12 weeks; (ii) partial EVR: a patient whose serum HCV RNA was reduced by 2-log or more of the HCV RNA before drug administration at 12 weeks, but who was not negative for serum HCV RNA; and (iii) non-EVR: a patient who was not classified as either cEVR or pEVR.

The patients were classified into the following three groups at the time of post-treatment at 24 weeks (final response): (i) sustained virological responder (SVR): a patient who was negative for serum HCV RNA during the six months following completion of the combination therapy; (ii) relapse (R): a patient whose serum HCV RNA was negative by the end of the combination therapy but reappeared after completion of the combination therapy; and (iii) virological non-responder (NR): a patient who was positive for serum HCV RNA during the entire course of the combination treatment.

RNA extraction

Liver biopsy specimens were stored in RNA later (Ambion, Austin, TX, USA) at -80°C until RNA

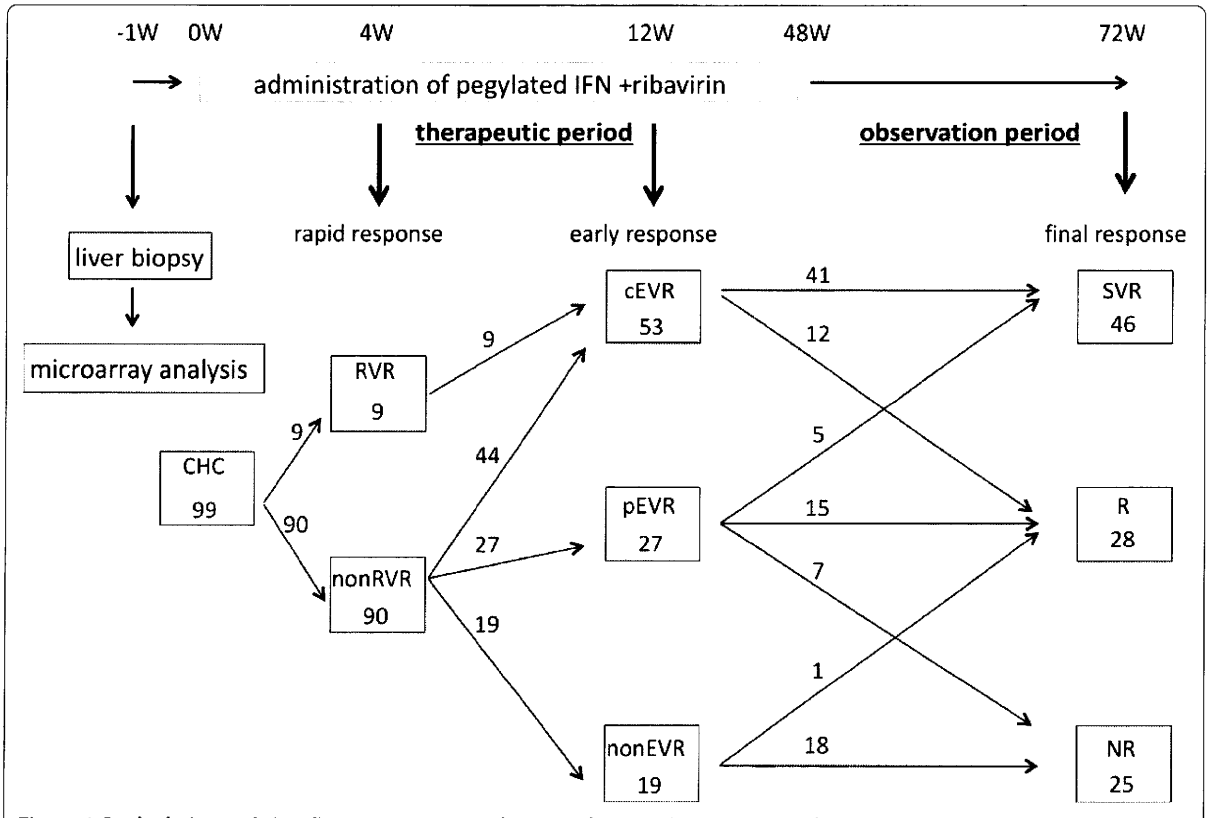

Figure 1 Study design and time-line response to combination therapy. The time-course of liver biopsy, microarray analysis, therapeutic period, observation period after combination therapy, and drug response judgment time (4W, 12W, 72W) is shown. Each therapeutic result (rapid, early, and final response) and the number of patients transitioning into each group are shown. RVR, cEVR, pEVR, SVR, R, and NR are denoted as rapid virological response, complete early virological response, partial EVR, sustained virological response, relapse, and non responder, respectively.

extraction. Total RNA was extracted by using mirVana™ miRNA Isolation kit (Ambion) according to the manufacturer's instruction.

miRNA microarray

miRNA microarrays were manufactured by using Agilent Technologies (Santa Clara, CA, USA). Total RNA (100 ng) were labeled and hybridized using a Human microRNA Microarray kit (Agilent Technologies) according to the manufacturer's protocol (Protocol for use with Agilent microRNA microarrays Version 1.5). Hybridization signals were detected using the DNA microarray scanner G2505B (Agilent Technologies), and all scanned images were analyzed using Agilent feature extraction software (v9.5.3.1). Data were analyzed using GeneSpring GX 7.3.1 software (Agilent Technologies) and normalized as follows: (i) values below 0.01 were set to 0.01. (ii) each measurement was divided by the 75th percentile of all measurements to compare one-color expression profiles. The data presented in this manuscript have been deposited in NCBI's Gene Expression Omnibus and are accessible through GEO Series accession number GSE16922: http://www.ncbi.nlm.nih.gov/geo/query/acc.cgi?token=xlmbxyyumcwkeba&acc=GSE16922

Real-time qPCR for miRNA quantification

To detect the expression level of miRNA by real-time qPCR, TaqMan® microRNA assay (Applied Biosystems) was used to quantify the relative expression levels of miR-18a (assay ID, 002422), miR-27b (assay ID, 000409), miR-422b (assay ID, 000575), miR-143 (assay ID, 000466), miR-145 (assay ID, 000467), miR-34b (assay ID, 000427), miR-378 (assay ID, 000567) and U18 (assay ID, 001204) which was used as an internal control. cDNA was synthesized by Taqman miRNA RT Kit (Applied Biosystems). Total RNA (10 ng) in 5 ul of nuclease free water was added to 3 ul of 5× RT primer, 10× 1.5 ul of reverse transcriptase buffer, 0.15 ul of 100 mM dNTP, 0.19 ul of RNase inhibitor, 4.16 ul of nuclease free water, and 50 U of reverse transcriptase in a total volume of 15 ul. The reaction was performed for 30 min at 16°C, 30 min at 42°C, and five min at 85°C. All RT reactions were run in triplicate. Chromo 4 detector (BIO-RAD, Hercules, CA, USA) was used to detect miRNA expression.

Method of predicting prognosis

Monte Carlo Cross Validation (MCCV) was used to identify a set of prognostic miRNAs and to assess and predict drug response [20,21]. We chose MCCV to make up for relatively small number of patients. The 99 enrolled patients were repeatedly and randomly divided 100 times into training sets (TSs; size n = 10, 20, ..., 90) and a corresponding validation set (VS; size = 99-n). The percentile-normalized measures for miRNA expression were compared between the 2 TS patient groups of SVR and non-SVR (R and NR) by computing absolute values of the difference for each of the 172 miRNAs that were higher than 10. A prognosis signature was defined in terms of the expression measures of the miRNAs with the largest absolute differences. A 35-miRNA prognosis predictor (PP) was established for TS patients and its performance was assessed on VS patients. A PP was computed by applying diagonal linear discriminant analysis to the 35-miRNA PP of the TS patients (Table 2 and 3). The PP was applied to predict the prognoses of the VS patients. The predicted and actual prognoses (SVR or non-SVR) of the VS patients were compared to obtain the following three measures of prognosis prediction performance: (1) accuracy (proportion of correctly predicted prognoses), (2) sensitivity (proportion of correctly predicted non-SVR) and (3) specificity (proportion of correctly predicted SVR). 53 patients (N and NR) were also repeatedly and randomly divided 100 times into training sets (TSs; size n = 6, 12, ...42) and corresponding validation set (VS; size = 53-n). Perl programs of our own writing performed all analytical processes.

Cell lines and miRNA transfection

HEK293 cells were maintained in D-MEM (Invitrogen, Carlsbad, CA, USA) with 10% fetal bovine serum, plated in 60 mm diameter dishes and cultured to 70% confluence. 293 cells were plated in 6-well plates the day before transfection and grown to 70% confluence. Cells were transfected with 50 pmol of Silencer® negative control siRNA (Ambion) or double-stranded mature miRNA (ds miRNA) or 2'-O-methylated antisense oligonucleotide against the miRNA of interest (ASO miRNA) (Hokkaido System Science, Sapporo, Japan) using lipofectamine RNAiMAX (Invitrogen). Cells were harvested 2 days after transfection.

Real-time qPCR for mRNA quanification

cDNA was synthesized using the Transcriptor High Fiderity cDNA synthesis Kit (Roche, Basel, Switzerland). Total RNA (2 μg) in 10.4 μl of nuclease free water was added to 1 μl of 50 mM random hexamer. The denaturing reaction was performed for 10 min at 65°C. The denatured RNA mixture was added to 4 μl of 5× reverse transcriptase buffer, 2 μl of 10 mM dNTP, 0.5 μl of 40 U/μl RNase inhibitor, and 1.1 μl of reverse transcriptase (FastStart Universal SYBR Green Master (Roche) in a total volume of 20 μl. The reaction ran for 30 min at 50°C (cDNA synthesis), and five min at 85°C (enzyme denaturation). All reactions were run in triplicate. Chromo 4 detector (BIO-RAD, Hercules, CA, USA) was used to detect mRNA expression. The primer sequences are as follows; BCL2 s; 5'-gttgctttacgtggcctgtt-3', as; 5'-ggaggtctggcttcatacca-3', RARA s; 5'-cataccctgccataccaacc-

Table 2 List of the 35 miRNAs used to classify patients into SVR and non-SVR groups using Monte Carlo Cross Validation (MCCV)

Gene name	fold change (SVR/non SVR)	T-test	Selection by MCCV		
			Rank	appearance frequency in this classification (%)	appearance number of times
hsa-miR-122a	1.32	6.67E-02	1	98.78	889
hsa-miR-21	1.19	3.62E-01	2	94.67	852
hsa-miR-22	1.23	7.80E-02	3	93.22	839
hsa-let-7a	1.14	3.57E-01	4	92.33	831
hsa-miR-23b	1.41	1.72E-02	5	91.44	823
hsa-miR-26a	1.32	7.45E-02	6	90.78	817
hsa-let-7f	1.15	4.04E-01	7	88.67	798
hsa-miR-142-3p	1.39	1.45E-01	8	87.33	786
hsa-miR-494	2.18	5.85E-03	9	82.00	738
hsa-miR-194	1.22	1.70E-01	10	80.78	727
hsa-let-7b	1.11	3.59E-01	11	80.22	722
hsa-miR-148a	1.25	2.28E-01	12	79.67	717
hsa-miR-29a	1.16	2.73E-01	13	77.78	700
hsa-miR-125b	1.20	2.37E-01	14	73.11	658
hsa-miR-192	1.09	4.89E-01	15	69.67	627
hsa-miR-24	1.25	8.31E-02	16	68.89	620
hsa-miR-768-3p	1.19	1.78E-01	17	68.78	619
hsa-miR-126	1.07	6.75E-01	18	49.56	446
hsa-miR-19b	1.15	2.98E-01	19	48.89	440
hsa-miR-370	2.00	1.44E-02	20	39.00	351
hsa-miR-29c	1.26	1.37E-01	21	38.89	350
hsa-miR-16	1.24	2.08E-01	22	37.11	334
hsa-miR-145	1.01	9.25E-01	23	34.89	314
hsa-let-7c	1.21	1.41E-01	24	33.22	299
hsa-miR-215	1.20	3.65E-01	25	27.67	249
hsa-let-7g	1.16	3.64E-01	26	27.44	247
hsa-miR-451	1.13	6.94E-01	27	23.11	208
hsa-miR-26b	1.30	2.26E-01	28	22.22	200
hsa-miR-92	1.12	3.44E-01	29	21.11	190
hsa-miR-29b	1.19	2.62E-01	30	19.44	175
hsa-miR-107	1.21	1.58E-01	31	18.78	169
hsa-miR-27b	1.40	2.32E-02	32	18.11	163
hsa-miR-638	1.32	5.57E-02	33	16.89	152
hsa-miR-199a*	1.12	5.92E-01	34	16.78	151
hsa-miR-193b	1.25	7.24E-02	35	16.67	150

3', as; 5'-gacatgaaaggagagtgggg-3', SMAD2 s; 5'-aatattttgg ggactgatgcc-3', as; 5'-gcttttgggcagtggttaag-3', and β-actin s; 5'-ccactggcatcgtgatggac-3', as; 5'-tcattgccaatggtgatgacct-3'. Assays were performed in triplicate, and the expression levels of target genes were normalized to the expression of the β-actin gene, as quantified using real-time qPCR as internal controls.

Statistical analysis

Data were statistically analyzed using the Student's t-test and differences in clinical characteristics among 3 groups were tested using the Kruskal-Wallis test, or Fisher's exact test. Data from microarray were also statically analyzed using Welch's test and Benjamini-Hochberg correction for multiple hypotheses testing.

Results

A microarray platform was used to determine miRNA expression of 470 miRNAs in 99 fresh-frozen CHC liver tissues.

miRNAs which related to the final response of combination therapy

Unique miRNA expression patterns were established according to the final virological response (SVR, R, and NR) to the combination therapy (Figure 1). To isolate

Table 3 List of the miRNAs used to classify patients into R and NR groups

Gene name	fold change (R/NR)	T-test	Selection by MCCV		
			Rank	appearance frequency in this classification (%)	appearance number of times
hsa-miR-122a	1.50	6.70E-02	1	98.57	690
hsa-miR-21	1.13	5.43E-01	2	89.86	629
hsa-let-7a	1.15	4.23E-01	3	88.71	621
hsa-let-7f	1.24	3.01E-01	4	87.43	612
hsa-miR-148a	1.70	4.51E-02	5	82.71	579
hsa-miR-192	1.24	1.93E-01	6	81.71	572
hsa-miR-126	1.21	3.19E-01	7	74.14	519
hsa-miR-22	1.04	7.88E-01	8	68.43	479
hsa-miR-194	1.20	3.63E-01	9	64.29	450
hsa-miR-23b	1.30	2.06E-01	10	62.00	434
hsa-miR-125b	1.23	2.88E-01	11	61.86	433
hsa-miR-494	0.45	8.17E-02	12	61.14	428
hsa-miR-19b	1.17	3.86E-01	13	61.14	428
hsa-miR-29a	1.11	5.44E-01	14	59.86	419
hsa-miR-26a	1.13	5.38E-01	15	58.43	409
hsa-let-7b	1.01	9.37E-01	16	56.86	398
hsa-miR-142-3p	1.15	5.54E-01	17	52.71	369
hsa-miR-215	1.28	3.93E-01	18	52.00	364
hsa-miR-101	1.31	1.26E-01	19	49.00	343
hsa-miR-451	1.35	5.25E-01	20	48.14	337
hsa-miR-145	0.99	9.76E-01	21	47.14	330
hsa-let-7g	1.15	4.84E-01	22	44.00	308
hsa-miR-29c	1.23	2.94E-01	23	43.71	306
hsa-miR-26b	1.37	2.85E-01	24	43.14	302
hsa-miR-768-3p	1.00	9.91E-01	25	36.29	254
hsa-let-7c	1.16	3.76E-01	26	36.14	253
hsa-miR-370	0.43	7.36E-02	27	35.57	249
hsa-miR-92	1.07	6.65E-01	28	34.14	239
hsa-miR-16	1.11	6.18E-01	29	26.71	187
hsa-miR-29b	1.14	5.19E-01	30	25.71	180
hsa-miR-27b	1.40	1.15E-01	31	25.71	180
hsa-miR-24	1.08	6.56E-01	32	20.57	144
hsa-miR-107	1.00	9.81E-01	33	19.57	137
hsa-miR-143	0.95	7.99E-01	34	18.43	129
hsa-miR-214	0.85	3.61E-01	35	17.86	125

the miRNAs that were associated with the drug response to the combination therapy, we chose miRNAs which had ≥ 1.25 fold difference in the mean values of the gene expression level between at least two groups ($p < 0.05$). Unsupervised hierarchical clustering based on all the miRNAs spotted on the chip, revealed a marked, very distinct separation according to the patients' final response of the CHC liver tissue to the Peg-IFN and ribavirin combination therapy (Figure 2).

The result was that the expression level of 3 miRNAs (miR-27b, miR-378, miR-422b) in SVR was significantly higher than that in NR, whereas the expression level of 5 miRNAs (miR-34b, miR-145, miR-143, miR-652, and miR-18a) in SVR was significantly lower than that in NR. Without FDR correction, the expression level of miR-122 in NR was lower than that in SVR. The expression level of 2 miRNAs in SVR was significantly higher than that in R, whereas the expression level of 10 miRNAs in SVR was significantly lower than in that in R. Additionally, the expression level of miR-148a in R was significantly higher than that in NR. There was no significant difference in the expression level of miR-122 in NR and R (Table 4).

Validation of the microarray result by real-time qPCR

The three miRNAs (miR-18a, miR-27b, and miR-422b) with the smallest difference of fold change between NR and SVR groups and four miRNA (miR-143, miR-145,

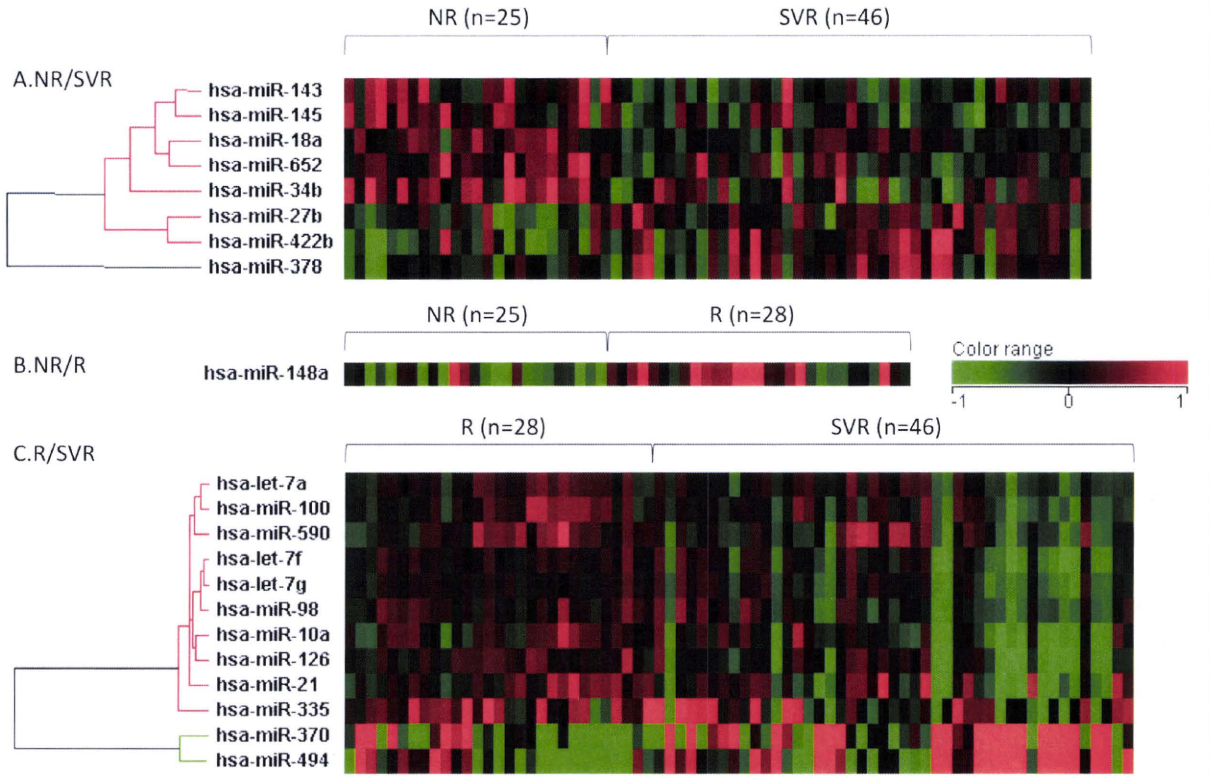

Figure 2 Clustering of CHC patients according to their final response to Peg-IFN and ribavirin combination therapy. Heatmap using miRNA differently expressed among SVR, R, and NR is shown (A: classification between NR and SVR, B: classification between NR and R, and C: classification between R and SVR, respectively). Vertical bars represent the miRNA genes and the horizontal bars represent the samples. Green bars reflect downregulated genes and red bars upregulated genes.

miR-34b, and miR-378) with the largest difference of fold change between NR and SVR groups were chosen to confirm the microarray results using stem-loop based real-time qPCR. The result of real-time qPCR corresponded to the result from the microarray analysis (Figure 3).

miRNAs which related to the 4 week (rapid response phase) response to combination therapy

The miRNA expression profile was established according to the rapid phase response to the combination therapy by week 4 (Table 5). Our results showed that the expression level of 5 miRNAs in non-RVR was significantly higher than that in RVR. Prior results have revealed that a patient who achieves RVR as a result of the combination therapy has a high possibility of achieving SVR [22,23]. Our research supports this finding: nine out of 99 patients achieved RVR. All nine cases shifted to cEVR by week 12, and 8 shifted to SVR at the final response. The 90 cases in non-RVR shifted to 44 cases in cEVR, 19 in pEVR, and 27 in non-EVR and at the final response shifted to 38 cases in SVR, 27 in R, and 25 in NR (Table 6 and Figure 1).

miRNAs which related to the 12 week (early response phase) response to combination therapy

Establishing the miRNA expression profile of patients according to their 12 week (early response) of CHC liver specimen to the combination therapy after 12 weeks, showed that the expression level of miR-23b and miR-422b in cEVR was higher than that in non-EVR, and the expression level of miR-34b in cEVR lower than that in non-EVR (Table 5). There were no miRNAs with expression level that differed significantly between cEVR and pEVR, and non-EVR and pEVR. The drug response at 12 weeks appeared to be a predictive factor of the final drug response. The 53 cases in cEVR at week 12 shifted to 41 cases in SVR and 12 in R at the final response. 27 cases in pEVR at week 12, shifted to 5 in SVR, 15 in R, and 7 in NR and 19 in non-EVR shifted to 1 in R and 18 in NR (Table 6 and Figure 1).

Predicting the final outcome before drug administration using MCCV

Before initial drug administration, we attempted to simulate the clinical outcome of the combination

Table 4 Extracted miRNA related to the final outcome of combination therapy

Gene Name	Fold Change (NR/SVR)	p-value with FDR correction	p-value without correction
hsa-miR-34b*	1.50	3.53E-02	6.95E-05
hsa-miR-145	1.35	3.55E-02	5.50E-05
hsa-miR-143	1.31	4.65E-02	6.46E-04
hsa-miR-652	1.28	4.33E-02	3.43E-04
hsa-miR-18a	1.22	4.33E-02	2.02E-05
hsa-miR-27b	0.78	4.33E-02	3.97E-05
hsa-miR-422b*	0.71	4.33E-02	1.44E-04
hsa-miR-378	0.70	4.86E-02	1.38E-03
hsa-miR-122	0.72	> 5.00E-02	2.59E-04

Gene Name	Fold Change (NR/R)	p-value with FDR correction	p-value without correction
hsa-miR-148a	0.59	1.60E-02	8.99E-04
has-miR-122	0.72	> 5.00E-02	6.23E-04

Gene Name	Fold Change (R/SVR)	P-value	p-value without correction
hsa-let-7a	1.15	3.93E-02	1.94E-03
hsa-let-7f	1.24	1.04E-02	3.60E-03
hsa-let-7g	1.17	1.93E-02	1.82E-02
hsa-miR-100	1.23	1.93E-02	9.23E-04
hsa-miR-10a	1.37	1.26E-02	2.40E-03
hsa-miR-126	1.36	1.04E-02	1.50E-03
hsa-miR-21	1.30	4.78E-02	3.45E-02
hsa-miR-335	2.00	2.83E-02	3.50E-02
hsa-miR-370	0.36	1.38E-02	2.96E-03
hsa-miR-494	0.37	3.93E-02	1.97E-03
hsa-miR-590	1.26	3.93E-02	5.59E-03
hsa-miR-98	1.22	1.38E-02	6.64E-03

Asterisk was denoted the common miRNAs appeared whose expression level between NR and SVR, and nonEVR and cEVR.

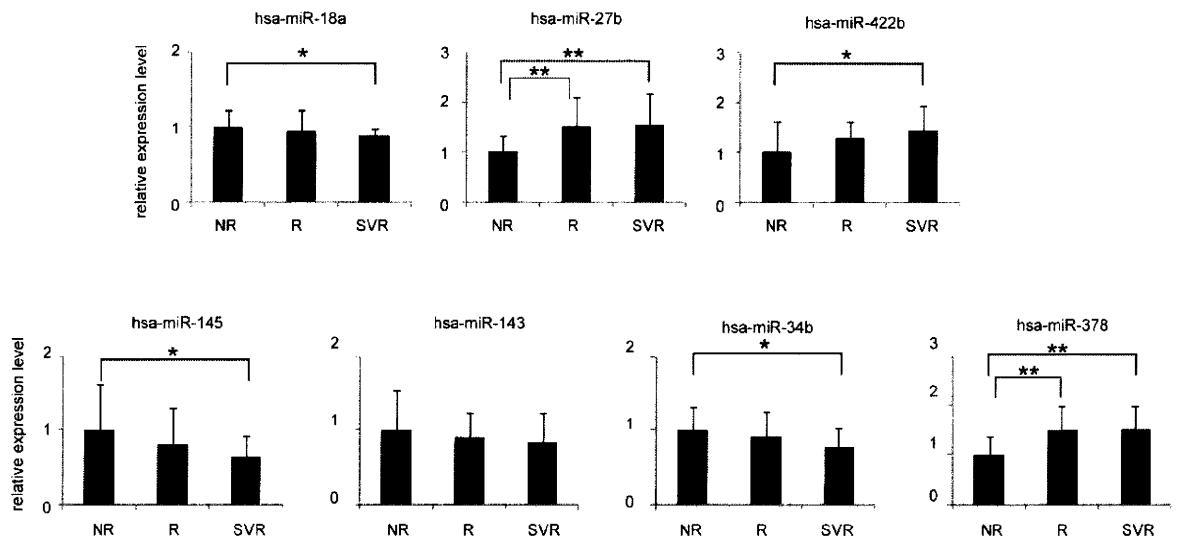

Figure 3 Real-time qPCR validation of the seven miRNAs. Each column represents the relative amount of miRNAs normalized to expression level of U18. The data shown were means+SD of three independent experiments. Asterisk indicates a significant difference of $p < 0.05$ (*) or $p < 0.01$ (**).

Table 5 List of the miRNA related to the rapid or early outcome of combination therapy

Gene Name	Fold Change (non RVR/RVR)	p-value	p-value without correction
hsa-let-7c	1.17	2.01E-02	8.31E-03
hsa-let-7d	1.13	3.50E-02	5.63E-02
hsa-miR-139	1.29	3.35E-02	2.70E-02
hsa-miR-324-5p	1.14	1.64E-02	3.24E-02
hsa-miR-768-5p	1.34	4.57E-02	1.29E-02

Gene Name	Fold Change (non EVR/cEVR)	p-value	p-value without correction
hsa-miR-34b*	1.51	3.30E-02	1.69E-04
hsa-miR-23b	0.74	2.69E-02	8.91E-05
hsa-miR-422b*	0.67	2.40E-02	1.34E-04
hsa-miR-122	0.74	> 5.00E-02	3.07E-03

Asterisk was denoted the common miRNAs appeared whose expression level between NR and SVR, and nonEVR and cEVR.

therapy before drug administration by using MCCV. We first extracted the SVR and non-SVR groups from all of the patients, and then the R and NR groups were predicted afterwards. MCCV simulation showed that the accuracy, specificity, and sensitivity of the liver specimen classified as SVR or non-SVR was up to 70.5%, 63.3%, and 76.8%, respectively (TSs = 80). On the other hand, the accuracy, specificity, and sensitivity of the liver specimen classified as R or NR was 70.0%, 73.7%, and 67.5%, respectively (TSs = 42)(Figure 4). Fold change of their normalized expression level, P value, and number of selection by MCCV in the 35 informative miRNAs that were identified based on the all patients are shown in Table 2 and 3.

miRNAs related to the final drug response can regulate the immune related genes

In order to clarify the biological links between miRNAs and IFN responses, we examined whether the expression of immune-related hypothetical miRNAs target genes (additional file 1) could be controlled by miRNAs which were related to the final drug response. We observed the changes in expression level of B-cell CLL/lymphoma 2 (BCL2), retinoic acid receptor, alpha (RARA), and SMAD family member 2 (SMAD2) by real-time qRT-PCR as the expression level of miRNAs (miR-143, miR-27b, and miR-18a) was modified, respectively, in HEK293 cells. The expression level of the hypothetical targets examined was down-regulated by over-expression of the corresponding miRNA and the corresponding antisense oligonucleotide (ASO) inhibited the function of miRNA (additional file 2).

Discussion

Our large and comprehensive screening revealed that hepatic miRNA expression can be associated with a patient's drug response. There are several reports that miRNAs are closely related to innate immunity, and in this study, we found that several miRNAs had the potential to recognize immuno-related genes as target candidates [24-26]. For example, the following hypothetical candidate genes of miR-378, miR-18a, miR-27b, miR-34b, and miR-145 each identified as target genes, Interferon Response Factor (IRF) 1, IRF2, IRF4, IRF6, and IRF7, respectively (additional file 1). Past reports show that miR-422b was related to the B cell differentiation [27]. When an immuno-reaction induces aberrant expression of miRNA, the expression level of miR-34b significantly decreased in H69 cells following IFN-γ stimulation [28]. Bcl-6 positively directs follicular helper T cell differentiation, through combined repression of miR-18a and miR-27b and transcription factors [29].

In our study, there was significant difference in the fold change of the expression level of miRNA based on the drug response, however, the absolute value of the fold change was not so significant (Table 4). Usually one miRNA can regulate many genes including immuno-related gene (additional file 1), and these genes in turn can synergistically affect immune activity. In our preliminary study (additional file 2) BCL-2, RARA, and SMAD2 can be regulated by miR-143, miR-18a, and miR-27b, respectively. Considering that the expression level of several miRNAs changed these minute changes taken together can have a significant impact on a patient's drug-response and innate immunity.

Aberrant expression of miRNA can modify the replication of HCV. According to Vita algorithm, several miRNAs, related to drug response, can recognize HCV genotype 1b sequence as a target (additional file 3) [30]. For example, miR-199a* is able to target the HCV genome and inhibit viral replication [12]. IFN has the ability to modulate expression of certain miRNAs that may either target the HCV RNA genome (miR-196 or miR-

Table 6 Patients' periodical drug response changes

code No.	4W treatment (rapid response)	12W treatment (early response)	48W treatment +24W observation (final outcome)	code No	4W treatment (rapid response)	12W treatment (early response)	48W treatment +24W observation (final outcome)
OCH-105	non RVR	non EVR	NR	OCH-103	RVR	cEVR	SVR
OCH-111	non RVR	pEVR	NR	OCH-104	non RVR	cEVR	SVR
OCH-118	non RVR	non EVR	NR	OCH-107	non RVR	cEVR	SVR
OCH-119	non RVR	non EVR	NR	OCH-108	non RVR	cEVR	SVR
OCH-122	non RVR	pEVR	NR	OCH-109	non RVR	cEVR	SVR
OCH-123	non RVR	non EVR	NR	OCH-110	non RVR	cEVR	SVR
OCH-126	non RVR	non EVR	NR	OCH-112	non RVR	pEVR	SVR
OCH-127	non RVR	non EVR	NR	OCH-114	RVR	cEVR	SVR
OCH-132	non RVR	pEVR	NR	OCH-116	non RVR	cEVR	SVR
OCH-137	non RVR	non EVR	NR	OCH-121	non RVR	pEVR	SVR
OCH-140	non RVR	pEVR	NR	OCH-124	non RVR	cEVR	SVR
OCH-142	non RVR	non EVR	NR	OCH-130	non RVR	cEVR	SVR
OCH-144	non RVR	pEVR	NR	OCH-131	non RVR	cEVR	SVR
OCH-145	non RVR	non EVR	NR	OCH-136	non RVR	cEVR	SVR
OCH-192	non RVR	non EVR	NR	OCH-138	non RVR	cEVR	SVR
OCH-204	non RVR	non EVR	NR	OCH-139	non RVR	cEVR	SVR
OCH-205	non RVR	non EVR	NR	OCH-143	non RVR	cEVR	SVR
OCH-206	non RVR	non EVR	NR	OCH-150	non RVR	cEVR	SVR
OCH-207	non RVR	non EVR	NR	OCH-153	non RVR	cEVR	SVR
OCH-208	non RVR	non EVR	NR	OCH-154	non RVR	cEVR	SVR
OCH-209	non RVR	pEVR	NR	OCH-155	non RVR	cEVR	SVR
OCH-210	non RVR	non EVR	NR	OCH-156	non RVR	cEVR	SVR
OCH-211	non RVR	non EVR	NR	OCH-157	non RVR	pEVR	SVR
OCH-223	non RVR	non EVR	NR	OCH-158	non RVR	pEVR	SVR
OCH-242	non RVR	pEVR	NR	OCH-160	non RVR	cEVR	SVR
OCH-101	non RVR	cEVR	R	OCH-186	non RVR	cEVR	SVR
OCH-102	RVR	cEVR	R	OCH-187	non RVR	cEVR	SVR
OCH-106	non RVR	non EVR	R	OCH-189	non RVR	pEVR	SVR
OCH-113	non RVR	pEVR	R	OCH-190	non RVR	cEVR	SVR
OCH-115	non RVR	cEVR	R	OCH-191	RVR	cEVR	SVR
OCH-117	non RVR	cEVR	R	OCH-194	non RVR	cEVR	SVR
OCH-120	non RVR	pEVR	R	OCH-195	non RVR	cEVR	SVR
OCH-125	non RVR	pEVR	R	OCH-222	non RVR	cEVR	SVR
OCH-128	non RVR	pEVR	R	OCH-228	non RVR	cEVR	SVR
OCH-129	non RVR	pEVR	R	OCH-229	RVR	cEVR	SVR
OCH-133	non RVR	pEVR	R	OCH-230	non RVR	cEVR	SVR
OCH-134	non RVR	pEVR	R	OCH-231	non RVR	cEVR	SVR
OCH-135	non RVR	cEVR	R	OCH-232	non RVR	cEVR	SVR
OCH-141	non RVR	cEVR	R	OCH-233	non RVR	cEVR	SVR
OCH-151	non RVR	pEVR	R	OCH-234	RVR	cEVR	SVR
OCH-152	non RVR	pEVR	R	OCH-236	non RVR	cEVR	SVR
OCH-159	non RVR	pEVR	R	OCH-237	non RVR	cEVR	SVR
OCH-188	non RVR	cEVR	R	OCH-238	non RVR	cEVR	SVR
OCH-213	non RVR	cEVR	R	OCH-240	RVR	cEVR	SVR
OCH-214	non RVR	pEVR	R	OCH-241	RVR	cEVR	SVR
OCH-215	non RVR	pEVR	R	OCH-243	RVR	cEVR	SVR
OCH-216	non RVR	cEVR	R				
OCH-217	non RVR	pEVR	R				
OCH-218	non RVR	cEVR	R				

Table 6: Patients?'? periodical drug response changes *(Continued)*

OCH-219	non RVR	pEVR	R
OCH-220	non RVR	cEVR	R
OCH-221	non RVR	pEVR	R
OCH-239	non RVR	cEVR	R

448) or markedly enhance its replication (miR-122) [10,11]. The low expression level of miR-122 in the subjects shown in the NR group is in accordance with our results, however, after miRNA expression profile with FDR correction, the expression level of miR-122 was not significantly different between SVR and NR groups [8]. One reason why this difference is that their study comprised of patients infected with HCV genotype from 1 to 4 while this study consisted of HCV genotype 1b patients only.

The expression pattern of mRNA in HCV infected liver tissue is different from that of healthy tissue [15]. The expression pattern of the IFN-related genes in liver tissue before administering of IFN therapy, also differs according to the drug response [15,19]. The amount of plasmacytoid dendritic cell (pDC), which are the most potent secretors of antiviral Type-I IFN, has been shown to decrease in the peripheral blood of patients, however, pDC tend to become trapped in the liver tissue if HCV infection is present [31,32]. Taken together, it is possible that the variation in the miRNA expression pattern according to the drug response existed even before therapy.

Previously, large randomized controlled trials of IFN therapy for CHC, identified at pre-treatment stage several possible factors which are associated with the final virological response. These factors include: genotype, amount of HCV RNA in peripheral blood, degree of fibrosis, age, body weight, ethnicity, and steatosis [33]. Viral genome mutation in the ISDR region and the

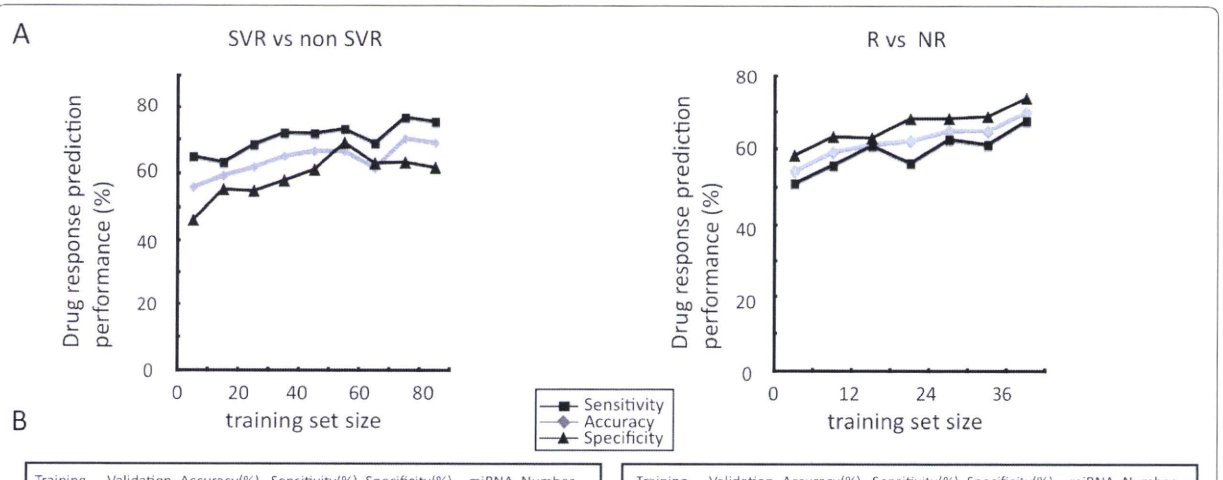

Training	Validation	Accuracy(%)	Sensitivity(%)	Specificity(%)	miRNA_Number
10	89	56.10	65.06	46.31	23
20	79	59.54	63.32	55.38	34
30	69	62.00	68.61	54.91	14
40	59	65.22	72.09	57.93	17
50	49	66.80	71.92	61.12	17
60	39	66.77	73.26	69.07	15
70	29	61.72	68.98	62.99	30
80	19	70.47	76.82	63.31	18
90	9	69.22	75.52	61.72	18

Training	Validation	Accuracy(%)	Sensitivity(%)	Specificity(%)	miRNA_Number
6	48	54.31	51.03	58.29	5
12	42	59.33	55.75	63.24	22
18	36	61.31	60.87	62.87	34
24	30	62.23	56.31	68.07	11
30	24	64.96	62.52	68.09	18
36	18	64.89	61.17	68.69	24
42	12	70.00	67.53	73.73	26

Figure 4 Method for predicting the clinical outcome using MCCV. Prediction performance of signatures from 35 miRNAs (Table 2 and 3). Left: Mean accuracy, specificity, and sensitivity (% in vertical axis) as a function of the training set size were determined for the 100 random splits of patients (non-SVR (NR+R) vs. SVR). Right: prediction performance of the training set size was determined by performing 48 random splits of patients (NR vs. R). A. Prediction performance (mean accuracy, specificity, and sensitivity) and number of miRNAs which was used for the prediction are also shown in each training set (TS) and validation set (VS).